Morphology and Mechanical and Viscoelastic Properties of Rubbery Epoxy/Organoclay Montmorillonite Nanocomposites

Amar Boukerrou,[1] Jannick Duchet,[2] Said Fellahi,[3] Mustapha Kaci,[1] Henry Sautereau[3]

[1]*Laboratoire des Matériaux Organiques, Université Abderrahmane Mira, Bejaia 06000, Algeria*
[2]*Laboratoire des Matériaux Macromoléculaires, 20 Avenue Albert Einstein, 69621 Villeurbanne-Lyon, France*
[3]*Intitut Algérien du Pétrole, Boumerdes 35000, Algeria*

ABSTRACT: The morphology and mechanical and viscoelastic properties of rubbery epoxy/organoclay montmorillonite (MMT) nanocomposites were investigated with wide-angle X-ray scattering (WAXS), transmission electron microscopy (TEM), tensile testing, and dynamic mechanical thermal analysis. An ultrasonicator was used to apply external shearing forces to disperse the silicate clay layers in the epoxy matrix. The first step of the nanocomposite preparation consisted of swelling MMT in a curing agent, that is, an aliphatic diamine based on a polyoxypropylene backbone with a low viscosity for better diffusion into the intragalleries. Then, the epoxy prepolymer was added to the mixture. Better dispersion and intercalation of the nanoclay in the matrix were expected. The organic modification of MMT with octadecy-lammonium ions led to an increase in the initial d-spacing (the $[d_{001}]$ peak) from 14.4 to 28.5 Å, as determined by WAXS; this indicated the occurrence of an intercalation. The addition of 5 phr MMTC18 (MMT after the modification) to the epoxy matrix resulted in a finer dispersion, as evidenced by the disappearance of the diffraction peak in the WAXS pattern and TEM images. The mechanical and viscoelastic properties were improved for both MMT and MMTC18 nanocomposites, but they were more pronounced for the modified ones. © 2006 Wiley Periodicals, Inc. J Appl Polym Sci 103: 3547–3552, 2007

Key words: mechanical properties; morphology; nanocomposites; organoclay; viscoelastic properties

INTRODUCTION

Polymer–clay nanocomposites are particulate-filled composites in which the reinforcement material is in the form of sheets with a thickness of one to a few nanometers and a length of hundreds to thousands of nanometers. Because of the high aspect ratio of the reinforcement, they show several advantages over typical composites in terms of the mechanical, thermal, physical, and barrier properties.[1] Among polymers, epoxy resins find many industrial applications in adhesives, construction materials, composites, laminates, coatings, and aircraft because of their high strength, low viscosity, low volatility, and low shrinkage during cure, low creep, and good adhesion to many substrates.[1] Therefore, epoxy resins are some of the most commonly studied polymers in the preparation of nanocomposites with layered silicates because the polar epoxy monomers can easily diffuse into the clay galleries.[2,3] In fact, the matrix/filler system, the extent of filler adhesion to the matrix, and

the levels of dispersion of the filler throughout the matrix are among the parameters that highly determine any enhancement of a particular property of nanocomposites.[4] Moreover, the nature of the curing agent and the curing conditions, especially the temperature, are expected to play a role in the exfoliation process.[2] In this respect, Kornmann et al.[5] reported that a long-chain alkylamine, having a chain of more than eight carbon atoms, could significantly result in an exfoliated clay structure. Furthermore, a balance between the intragalleries and the extragallery polymerization rates is essential for exfoliating the clay into an epoxy system.[6] According to literature data,[7–11] there are three different methods to synthesize polymer–clay nanocomposites: a melt-intercalation process for thermoplastic polymers; a solution method in which both the organoclay and polymer precursor are dissolved in a polar organic solvent, and an *in situ* polymerization technique. The last is the most effective technique for thermoset polymer matrix nanocomposites.[6]

On the other hand, the commonly used techniques for processing clay–epoxy nanocomposites are direct mixing and solution mixing.[12] However, these two techniques produce intercalated or intercalated/exfoliated composites rather than fully exfoliated compo-
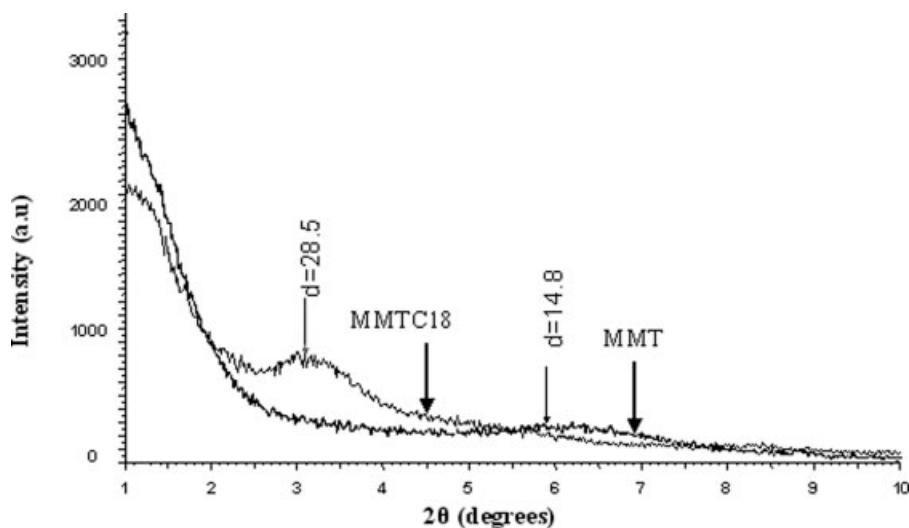
Figure 1 Wide-angle X-ray diffraction patterns of unmodified MMT and MMTC18. The distance is given in angstroms.

sites. According to Vaia et al.,[13] the degree of exfoliation can be improved through the aid of conventional shear devices such as extruders, mixers, and ultrasonicators.

In this study, ultrasonicators were used as a means of applying external shearing forces to enhance the dispersion of the silicate clay in the matrix. Initially, the procedure consisted of swelling the clays in a curing agent of a low viscosity for better diffusion into the intragalleries. Then, the epoxy prepolymer was added. Under these conditions, the occurrence of a better dispersion was expected. The ultrasonic process was used to improve the breakup of layered silicate bundles and further reduce the dispersion size with better homogeneity.[14]

Therefore, the objective of this work was the preparation of nanocomposites based on diglycidyl ether of bisphenol A (DGEBA)/Jeffamine D2000 modified montmorillonite (MMT) clay by an ultrasound-assisted mixing process. The morphology and mechanical and thermomechanical properties were investigated with wide-angle X-ray scattering (WAXS), transmission electron microscopy (TEM), tensile analysis, and dynamic mechanical thermal analysis. The results were compared with those of the unmodified nanocomposites and the neat matrix.

EXPERIMENTAL

Materials

The clay was a natural MMT that originated from the region of Maghnia in Algeria, and it was kindly supplied by Algerian Enterprise (ENCG, Bejaia, Algeria). It was an aluminous silicate containing Fe, Ca, Mg, Na, and K according to the following chemical structure: $Na_{0.19}K_{0.20}Ca_{0.04}(Mg_{0.36}Fe_{0.10}Al_{1.44})Si_4O_{10}(OH)_2$. The cation exchange capacity of the clay was 110 mequiv/100 g.
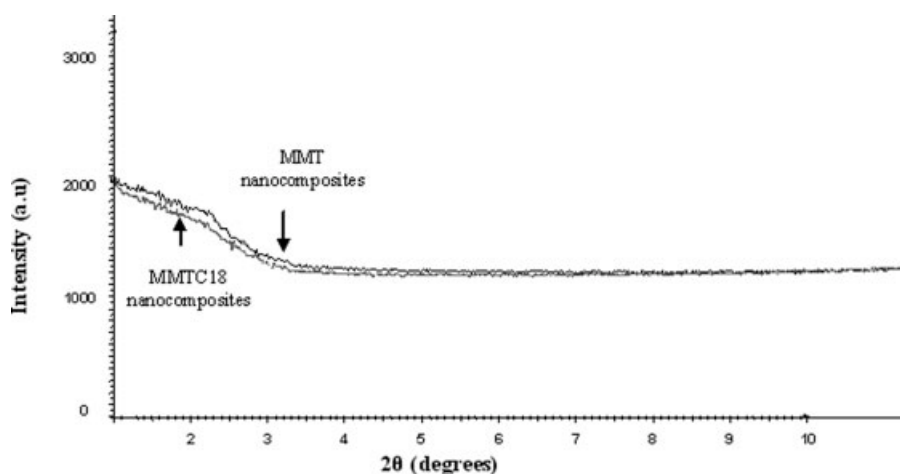
Figure 2 Wide-angle X-ray diffraction patterns of DGEBA/D2000/MMT and DGEBA/D2000/MMTC18 nanocomposites. The distance is given in angstroms.
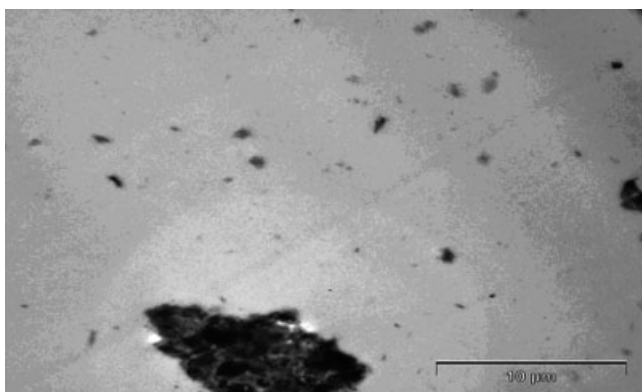
Figure 3 TEM image of the DGEBA/D2000/MMT nanocomposites.

The organic system was based on epoxy/amine; the prepolymer DGEBA was manufactured by Vantico (Paris, France) under the trade name DGEBA LY 556 with the following characteristics: an *n* (polymerization degree) value of 0.15 and a number-average molecular weight of 382.6 g/mol. The curing agent was an aliphatic diamine with a polyoxypropylene backbone supplied by Huntsman (Everberg, Belgium) under the trade name Jeffamine D2000 with a number-average molecular weight of 1970 g/mol.

Organoclay preparation

The method of organoclay preparation was similar to that used by Le Pluart.[15] The silicates were exchanged with octadecylammonium ions at 80°C with two cation exchange capacity (amine/clay ratio). Octadecylamine (0.2 mol) was dissolved in 20 L of a 0.01*N* hydrochloric acid solution (based on deionized water). The solution was stirred at 80°C for 3 h. Then, 100 g of clay was added to the solution, and the whole was stirred at the same temperature for 3 h more. The solution was filtered, and the silicates were further washed six more times with hot deionized water and one time with a hot ethanol/water (1 : 1) mixture so that no chloride

would be detected upon the addition of 0.1 mol/L aqueous $AgNO_3$.

The resulting organoclay was then dried at 85°C for 36 h and kept dry in a vacuum box. After the modification, the organoclay was known as MMTC18.

Preparation of the epoxy nanocomposites

The silicate clays (5 phr) and the curing agent were initially sonicated at 80°C for 10 min with an ultrasonic processor device at a frequency of 20 kHz and an amplitude of 6 μm. The temperature of 80°C corresponded to the first curing temperature of the reactive agents. The epoxy prepolymer was then added to the mixture, and the whole was stirred for 15 min more. Then, the blend was poured into a steel mold and cured for 2 h at 80°C; this was followed by a postcure for 3 h at 125°C. The stoichiometric mass ratio of DGEBA to D2000 was calculated, and the value was 2.65 according to the diamine functionality, which was itself determined by chlorydric acid in dioxane (3.54).[16]

Nanocomposite characterization

WAXS

WAXS measurements were performed at room temperature on a Siemens D500 diffractometer (Germany) with a Brentano Bragg geometry goniometer with Cu Kα radiation (wavelength = 1.54 Å) operating at 40 kV and 30 mA. The diffraction patterns were collected between 2θ angles of 1 and 10° at a scanning rate and step size of 5°/min and 0.02°, respectively.

TEM

The different nanocomposites samples were ultramicrotomed with a diamond knife on a Leica (Bannockburn, IL) Ultracut UCT microtome at −70°C to give sections with a nominal thickness of 70 nm. The sections were transferred from dry conditions (−70°C) to car-

Figure 4 TEM image of the DGEBA/D2000/MMTC18 nanocomposites.
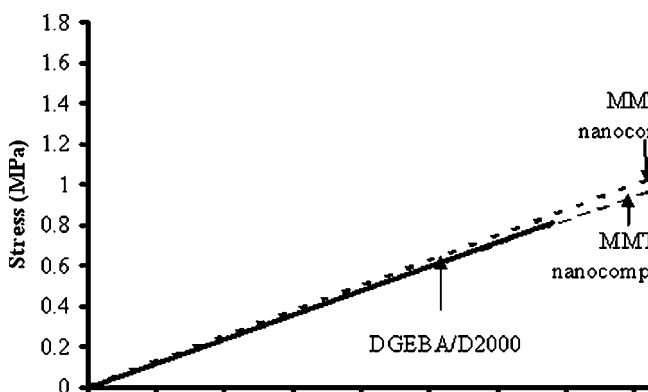
Figure 5 True stress–strain parameters of the DGEBA/D2000 matrix and MMT and MMTC18 nanocomposites.

TABLE I
Mechanical Properties of the Nanocomposites Based on the DGEBA/D2000 Matrix

DGEBA/D2000 matrix	G (MPa)	G/G_0	σ_r (MPa)	ε_r (%)	W_b (10^{-3} J)	W_b/W_0
Unloaded	0.56	1	0.8 ± 0.048	69 ± 5.78	26 ± 3	1
MMT (5 phr)	0.61	1.07	0.95 ± 0.048	83 ± 2.71	43 ± 2	1.65
MMTC18 (5 phr)	0.78	1.36	1.11 ± 0.045	91 ± 3.16	61 ± 5	2.34

G_0, elastic modulus of the neat matrix; ε_r, elongation at break; W_0, energy at break of the neat matrix; W_b, energy at break of the nanocomposite; σ_r, stress at break.

bon-coated, 200-mesh Cu grids. The TEM images were obtained at 120 kV under low dose conditions with a Philips CM120 electron microscope (The Netherlands).

Tensile testing

The stress–strain parameters were measured according to the NF T 51-034 method on a 2/M tensile machine belonging to the MTS Society (Toulouse, France). The specimen had the shape H3 with the dimensions $2 \times 4 \times 10$ mm^3, and the measurements were carried out at room temperature with a crosshead speed of 5 mm/min. An average value of five samples was determined.

The theory of rubber elasticity[17] was used to relate the deformation state at the molecular level to the externally applied deformation. In the case of uniaxial deformation, the true stress (σ; the force divided by the deformed area) is defined for dry networks formed in the bulk state as

$$\sigma = (\rho RT/M_c) \times (\lambda^2 - \lambda^{-1})$$

where ρ is the network density, R is K. Na, T is the absolute temperature, M_c is the average molecular weight of chains between crosslinks, and λ is the extension ratio defined as the ratio of the final length of the sample in the direction of stretch to the initial length before deformation.

Dynamic mechanical thermal analysis

The dynamic mechanical thermal analysis of the nanocomposite properties was determined with a Rheometrics dynamic analyzer (Paris, France). The tests were carried out in the torsion deformation mode at a frequency of 1 Hz with a temperature program ranging from -100 to $50°C$ at a heating rate of $3°C/min$ under a controlled strain of 0.17% corresponding to the linear portion of the viscoelastic domain of the material.

RESULTS AND DISCUSSION

Morphology

Figure 1 shows the XRD patterns for both MMT and MMTC18 in the 2 θ region of 1–10°. The formation of a very broad peak can be observed at almost 2 θ = 6.5°, corresponding to a d-spacing of 14.4 Å, for MMT; it is

assigned to the [001] lattice spacing of the unmodified clay. After MMT modification with octadecylammonium ions, the initial d-spacing increases from 14.4 to 28.5 Å. The swelling of the gallery layers is generally interpreted as the result of the organic modification of MMT involving cationic exchange between ions of MMT and those of alkyl ammonium.[18]

Figure 2 exhibits the XRD patterns of DGEBA/D2000/MMT and DGEBA/D2000/MMTC18 nanocomposites. The XRD patterns of the unmodified and modified nanocomposites are similar, and no peak has been detected.

Figures 3 and 4 show TEM images of MMT and MMTC18 nanocomposites, respectively. In Figure 3, the formation of agglomerates clearly indicates the poor dispersion of the clays in the epoxy matrix. In contrast, Figure 4 illustrates a better dispersion of the clay particles and layers in the matrix resulting from the swelling of MMTC18 in the nanocomposites.

Mechanical properties

Figure 5 shows the stress–strain curves for the epoxy matrix and MMT and MMTC18 nanocomposites. An increase in both the stress and the strain at break can be observed for both nanocomposite samples in comparison with the epoxy matrix. In fact, the stress at break increases by 20% for MMT and by 40% for MMTC18. Similar behavior has also been noted in the case of strain at break: increases of 20 and 32% have been
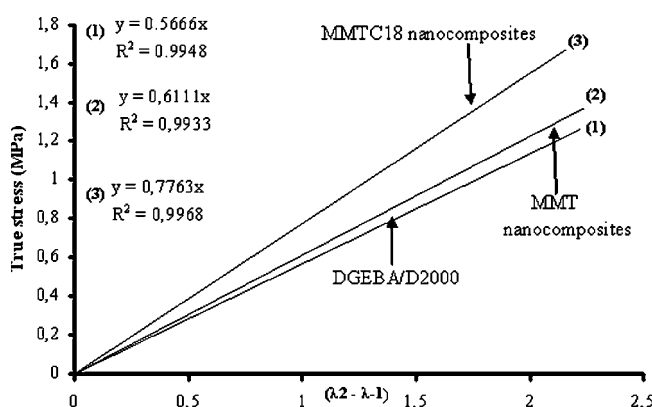
Figure 6 True stress as a function of $\lambda^2 - \lambda^{-1}$ for the DGEBA/D2000 matrix and MMT and MMTC18 nanocomposites.
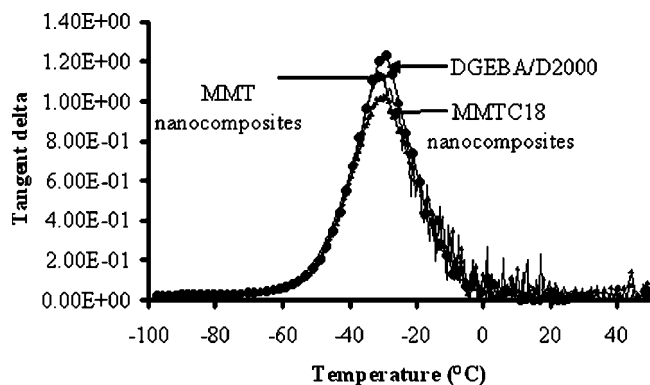
Figure 7 Tan δ as a function of temperature for the DGEBA/D2000 matrix and MMT and MMTC18 nanocomposites.

Formulation	G' at 25°C (GPa)	T_m (°C)	Tan δ
DGEBA/D2000	1.43	−31	1.2
MMT/DGEBA/D2000	1.81	−30	1.1
MMTC18/DGEBA/D2000	1.93	−29	1.0

found for the unmodified and modified clay nanocomposites, respectively (Table I). The increase in these two parameters could be attributed to better dispersion of organophilic clay in the nanocomposites.[19,20] These results are in agreement with those obtained by TEM.

Figure 6 shows the curves of the true stress as a function of $\lambda^2 - \lambda^{-1}$ for the epoxy matrix and MMT and MMTC18 nanocomposites. The general shape of the curves fits well a linear relationship that is described by the following equation: $\sigma = G(\lambda^2 - \lambda^{-1})$, where G represents the slope of the curve, which is defined as the rubber elasticity modulus.[17] In both samples, the stiffness is improved, but it is more pronounced for the MMTC18 samples. Indeed, this characteristic is improved by 10 and 40% for MMT and MMTC18 nanocomposites, respectively. This result is consistent with the data reported by Pinnavaia et al.[21] and Wang and Pinnavaia,[22] who indicated that the addition of 5 wt % MMT to an epoxy amine matrix led to a twofold increase in the rubber elasticity of the nanocomposites compared with that of the matrix. The G values are also reported in detail in Table I.
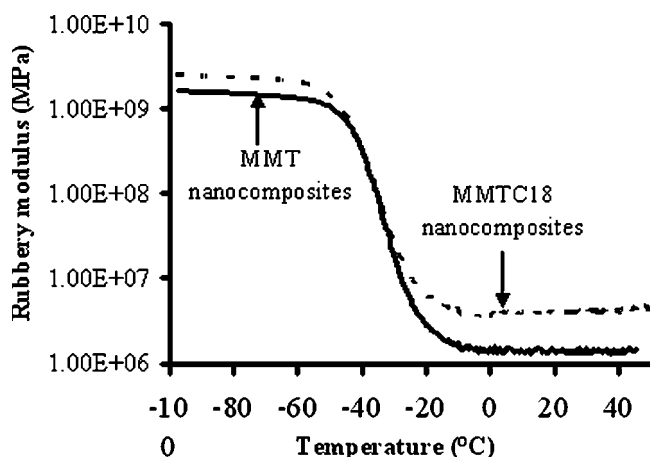
Figure 8 Storage modulus, measured at 1 Hz, as a function of temperature for the DGEBA/D2000 matrix and MMT and MMTC18 nanocomposites.

Dynamic thermal mechanical properties

The dynamic mechanical properties of MMT and MMTC18 nanocomposites were studied over a wide temperature range (−100 to 50°C). The variation of tan δ as a function of temperature for both nanocomposites is shown in Figure 7. One relaxation peak corresponds to the mechanical transition temperature, which slightly decreases in the presence of the organoclay. According to the literature,[23] this behavior is attributable to a reduction in the polymer volume fraction due to the presence of the filler. This means that at a low temperature, the polymer matrix by itself is responsible for a high proportion of energy dissipation, whereas the nanoparticles strongly absorb any energy.

Figure 8 shows the storage modulus (i.e., the elastic modulus) of MMT and MMTC18 nanocomposites as a function of temperature. The organoclay induces a slight increase in the modulus. All the data are given in detail in Table II.

CONCLUSIONS

From this study, the following conclusions can be drawn. The modification of the MMT surface by octadecylammonium ions leads to an intercalation, as revealed by WAXS analysis. The addition of 5 phr MMTC18 to the matrix and the use of ultrasound-assisted mixing result in a better dispersion of the nanofiller. As a result, an improvement in both the stress–strain parameters at break and the viscoelastic properties is obtained. Finally, MMTC18 considerably increases both the stiffness and energy at break of nanocomposites, even though it is not easy to obtain a compromise between the two parameters. In our case, the homogeneity of the morphology induces significant increases in both the stiffness and the energy at break of roughly 40% and more than 100%, respectively.

References

1. Isik, I.; Yilmazer, U.; Bayram, G. Polymer 2003, 44, 6371.
2. Kornmann, X.; Lindberg, H.; Berglund, L. A. Polymer 2001, 42, 4493.

3. Chin, I. J.; Thurn-Albrecht, T.; Kim, H. C.; Russel, T. P.; Wang, J. Polymer 2001, 42, 5947.
4. Evora, V. M. F.; Shukla, A. Mater Sci Eng A 2003, 363, 358.
5. Kornamn, X.; Lindberg, H.; Berglund, R. A. Polymer 2001, 42, 1303.
6. Nigam, V.; Setua, D. K.; Matur, G. N.; Kar, K. K. J Appl Polym Sci 2004, 93, 2201.
7. Mascia, L.; Prezzi, I. Adv Polym Technol 2005, 24, 91.
8. Mascia, L.; Prezzi, I.; La Vormia, M. Polym Eng Sci 2005, 45, 1039.
9. Kinloch, A. J.; Lee, J. H.; Taylor, A. C.; Sprenger, S.; Eger, C.; Egan, D. J Adhes 2000, 79, 867.
10. Alexandre, M.; Dubois, P. Mater Sci Eng 2000, 28, 1.
11. Park, J.; Jana, S. C. Macromolecules 2003, 36, 6391.
12. Asma, Y.; Jandro, L. A.; Issac, M. D. Scr Mater 2003, 40, 81.
13. Vaia, R. A.; Jandt, K. D.; Kramer, E. J.; Giannelis, E. P. Chem Mater 1996, 8, 2628.
14. Ryu, J. G.; Kim, H.; Lee, J. W. Polym Eng Sci 2004, 44, 1198.
15. Le Pluart, L. Ph.D. Thesis, Institut National des Sciences Appliquées (INSA), Lyon, France, 2002.
16. Lan, T.; Pinavaia, T. J. Chem Mater 1994, 6, 2216.
17. Bokobza, L. Macromol Symp 2001, 171, 163.
18. Le Pluart, L.; Duchet, J.; Sautereau, H.; Gerard, J. F. J Adhes 2002, 78, 645.
19. Lee, K. Y.; Goettler, L. A. Polym Eng Sci 2004, 44, 1103.
20. Le Pluart, L.; Duchet, J.; Sautereau, H. Polymer 2005, 46, 12267.
21. Pinnavaia, T. J.; Lan, T.; Karavatina, P. D.; Wang, Z.; Shi, H. Am Chem Soc Polym Mater Sci Eng 1996, 74, 117.
22. Wang, Z.; Pinnavaia, T. J. Chem Mater 1998, 10, 1820.
23. Wang, M. J. Rubber Chem Technol 1998, 71, 520.